

# Fluids in porous media: The case of neutral walls

Giuseppe Pellicane,<sup>1,2</sup> Richard L. C. Vink,<sup>3</sup> Bruno Russo,<sup>4</sup> and Paolo V. Giaquinta<sup>5</sup>

<sup>1</sup>*School of Chemistry and Physics, University of Kwazulu-Natal,  
Private Bag X01, Scottsville 3209, Pietermaritzburg, South Africa*

<sup>2</sup>*National Institute for Theoretical Physics (NITheP), KZN node, Pietermaritzburg, South Africa*

<sup>3</sup>*Institute of Theoretical Physics, Georg-August-Universität,  
Friedrich-Hund-Platz 1 D-37077 Göttingen, Germany*

<sup>4</sup>*Techimp Corporate Headquarter, Via Toscana, 11/c, 40069 Zola Predosa (BO), Italy*

<sup>5</sup>*Dipartimento di Fisica e di Scienze della Terra, Università degli Studi di Messina,  
Viale F. Stagno d'Alcontres 31, 98166 Messina, Italy*

(Dated: January 23, 2021)

The bulk phase behavior of a fluid is typically altered when the fluid is brought into confinement by the walls of a random porous medium. Inside the porous medium, phase transition points are shifted, or may disappear altogether. A crucial determinant is how the walls interact with the fluid particles. In this work, we consider the situation whereby the walls are neutral with respect to the liquid and vapor phase. In order to realize the condition of strict neutrality, we use a symmetric binary mixture inside a porous medium that interacts identically with both of the mixture species. Monte Carlo simulations are then used to obtain the phase behavior. Our main finding is that, in the presence of the porous medium, a liquid-vapor type transition still occurs, but with critical exponents that deviate from bulk Ising values. In addition, we observe clear violations of self-averaging. These findings provide further evidence that random confinement by neutral walls induces critical behavior of the random Ising model (i.e. Ising models with dilution type disorder, where the disorder couples to the energy).

PACS numbers: 05.70.Jk (critical point phenomena), 64.70.Fx (liquid-vapor transitions), 02.70.-c (computational techniques; simulations)

## I. INTRODUCTION

The confinement of a fluid to the voids of a porous material generally influences the critical behavior of the fluid. For example, lutidine-water mixtures in Vycor [1], or <sup>4</sup>He [2], nitrogen [3] and carbon dioxide [4] in silica aerogel, yield critical exponents of their associated liquid-vapor transitions that differ profoundly from bulk values (the bulk exponents typically being those of the three-dimensional Ising model). One line of thought is that the random pore structure induces quenched spatial fluctuations in the chemical potential [5]. This conjecture, originally put forward by de Gennes [6], implies that the critical behavior of the fluid inside the pores should be that of the random-field Ising model (RFIM) [7, 8]. Recent simulations of fluids inside porous media have indeed uncovered critical behavior characteristic of the RFIM [9–12]. In order for RFIM universality to arise, it is crucial that the pore walls feature a preferred attraction to one of the fluid phases. This condition is typically fulfilled in experiments, as one of the phases, i.e. the liquid or the vapor, is frequently seen to wet the pore walls [1, 3, 4].

Nevertheless, for our fundamental understanding of fluid phase behavior, the situation of “neutral” pore walls which do not preferentially attract, is of interest also. A different universality class is then expected to come into play [13, 14], namely the one of the random Ising model (RIM). The defining feature of the RIM is that the quenched randomness of the porous medium couples to the energy (as opposed to the order parameter in the

RFIM). Typical lattice models that belong to the universality class of the RIM are the site-diluted Ising model and the random-bond Ising model [15]. In  $d = 3$  dimensions, the Harris criterion [16] implies that the RIM should still feature a liquid-vapor critical point, but with critical exponents different from those of the bulk Ising model, since the latter has a positive specific heat critical exponent (by bulk we mean in the absence of the porous medium). However, the difference in the critical exponents between bulk Ising and RIM universality is very small, and challenging to detect numerically [15]. In contrast, the difference between bulk Ising and the RFIM is much more pronounced, since hyperscaling is violated in the latter. In  $d = 3$  dimensions, this yields a very pronounced numerical signature which one can easily detect in simulations [8–11].

Regarding the case of a fluid confined to a neutral porous medium, the question of whether this system exhibits RIM universality was recently addressed in simulations [14]. As expected for the RIM, these simulations revealed a critical point, located at an increased density compared to the bulk. By carefully measuring the critical amplitude ratio of the susceptibility, these simulations also uncovered deviations from bulk Ising behavior, and toward that of the RIM. The aim of this work is to corroborate these findings, using a more sophisticated (grand-canonical) simulation scheme, larger system sizes, as well as additional finite-size scaling methods. In particular, we will address the question of self-averaging. The presented analysis provides further support of RIM universality in fluids confined to neutral pores.

The outline of this paper is as follows: In Section II, we introduce the model for the fluid mixture and for the porous medium with neutral walls, and we describe the simulation method. The results are presented in Section III, and we end with a discussion in Section IV.

## II. MODEL AND METHODS

### A. Model: fluid inside neutral porous medium

We consider the same model as in Ref. 14, which is a fluid confined to a neutral porous medium in  $d = 3$  spatial dimensions. It belongs to the family of “quenched-annealed” mixtures [17, 18], which are routinely used to model fluids inside pores [9, 13, 19–28]. The fluid is a non-additive binary mixture of spheres, species  $A$  and  $B$ , of equal diameter  $\sigma$  (in what follows  $\sigma$  is the unit of length). The particles interact via hard-sphere pair potentials

$$\begin{aligned} u_{AA}(r) = u_{BB}(r) &= \begin{cases} \infty & r < \sigma \\ 0 & \text{otherwise,} \end{cases} \\ u_{AB}(r) &= \begin{cases} \infty & r < (1 + \Delta)\sigma \\ 0 & \text{otherwise,} \end{cases} \end{aligned} \quad (1)$$

with  $r$  the center-to-center distance between a pair of particles, and  $\Delta$  the non-additivity parameter. The porous medium is a fixed configuration of non-overlapping spheres, species  $M$ , also of diameter  $\sigma$ . These spheres are distributed randomly at the start of the simulation, at density  $\rho_M$ , but remain immobile (quenched) thereafter. Only after the porous medium has been generated, are the (mobile) fluid particles inserted. Note that Eq. (1) is symmetric under the exchange of particle labels  $A \leftrightarrow B$ . In order to retain this symmetry, the medium particles  $M$  interact symmetrically with the mobile fluid particles:  $u_{AM}(r) = u_{BM}(r) \equiv u_{AA}(r)$ . In this way, we ensure that the porous medium remains neutral, i.e. does not preferentially attract one of the fluid species. As a consequence, we do *not* expect the critical behavior of the RFIM for this system.

For  $\Delta > 0$ , the model of Eq. (1) exhibits a liquid-vapor type transition [29]. To analyze this transition later on, we introduce the overall fluid density  $\rho = (N_A + N_B)/V$ , and the composition (order parameter)

$$m = (N_A - N_B)/V, \quad (2)$$

where  $N_\alpha$  is the number of particles of species  $\alpha$ , and  $V$  the volume of the system. Provided  $\rho > \rho_{\text{cr}}$ , two fluid phases are observed, I and II, characterized by a positive and negative composition,  $m_I$  and  $m_{II}$ , respectively (due to symmetry  $m_I = -m_{II}$ ). Precisely at  $\rho = \rho_{\text{cr}}$ , the system becomes critical, where  $m_I = m_{II} = 0$ . We emphasize that  $\rho_{\text{cr}}$  is not trivially known beforehand (its value depends on  $\Delta$  and  $\rho_M$ ). For  $\rho < \rho_{\text{cr}}$ , the system

reveals only one phase. Of course, this behavior is analogous to that of the Ising model, if one identifies  $m$  in Eq. (2) as the magnetization per spin [30, 31].

Our model is thus defined by the non-additivity parameter  $\Delta$ , and the density of the porous medium  $\rho_M$ . In what follows,  $\Delta = 0.2$ , while for the porous medium  $\rho_M = 0.1$  and  $0.2$  will be considered, as well as the bulk situation  $\rho_M = 0$ .

### B. Method: grand-canonical Monte Carlo

Our simulations are performed in the grand-canonical (GC) ensemble, where the volume  $V$  is constant, while the particle numbers  $N_\alpha$  can fluctuate freely, as governed by the fugacity  $z_\alpha$ . Here,  $\alpha \in \{A, B\}$  strictly refers to the mobile fluid, since the porous medium is quenched. Due to the symmetry of the model, it follows that  $N_A = N_B$  at criticality, and so we set the particle fugacities equal:  $z_A = z_B \equiv z$ . The corresponding Boltzmann weight of a given particle configuration  $w \propto z^{N_A + N_B} e^{-E/k_B T}$ , with  $E$  the potential energy given by Eq. (1),  $T$  the temperature, and  $k_B$  the Boltzmann constant. Of course, for hard spheres,  $T$  does not affect static equilibrium properties, and thus is irrelevant. The sole control parameter in our simulations is therefore the fugacity  $z$ . In this work, we use standard single particle Monte Carlo moves [32] to generate particle configurations conform the weight  $w$ . To enhance efficiency, histogram reweighting is used to extrapolate data obtained for one value of  $z$  to different (nearby) values [33]. The simulations are performed in a cubic box of edge  $L$  with periodic boundaries.

The principal output of the simulations is the (normalized) distribution

$$P(m) \equiv P(m|z, L, \rho_M), \quad \int_{-\infty}^{\infty} P(m) dm = 1, \quad (3)$$

defined as the probability to observe the system in a state with composition  $m$ , with  $m$  given by Eq. (2). We emphasize that  $P(m)$  depends on all the system parameters, in particular the fugacity  $z$ , and the system size  $L$ . Note also that, due to symmetry,  $P(m) = P(-m)$ , and that this symmetry holds irrespective of whether a porous medium is present.

To facilitate a finite-size scaling analysis (both for the bulk system, and inside the porous medium) four different system sizes were simulated:  $L/\sigma = 13.57; 17.07; 20.57; 24.07$  (in the figure legends, we report the system size rounded down to the nearest integer). For these system sizes, the total number of mobile particles ranged between  $\sim 1200 - 6000$ . The simulations were equilibrated for at least  $10^5$  GC cycles, and averages were obtained following production runs of  $10^6 - 10^7$  GC cycles (longer runs were performed for state points close to the critical point). A GC cycle consists of a number of attempted MC steps equal to the average total number of particles in the system.

TABLE I: Critical exponents  $\beta$ ,  $\gamma$  and  $\nu$  of the universality class of the bulk Ising model, and the random Ising model (RIM) taken from various references [15, 34]. The spatial dimension  $d = 3$ .

	$\beta$	$\gamma$	$\nu$
Ising	0.326	1.237	0.630
RIM	0.354	1.341	0.683

For the fluid mixture inside the porous medium,  $\rho_M > 0$ , results were additionally averaged over at least  $M = 100$  different configurations of the porous medium. The medium configurations were generated by equilibrating a system of hard spheres at fixed density  $\rho_M$  using canonical Monte Carlo moves for at least  $10^6$  cycles (here a cycle is defined as one attempted move per particle; as canonical move we used random displacements of single particles). After equilibration,  $M$  configurations were collected and stored at intervals of  $10^5$  cycles. Then, the mobile  $AB$  particles of the fluid binary mixture were randomly inserted in the hollow cavities of the porous medium, and the distribution  $P(m)$  of Eq. (3) was obtained in productions runs lasting  $10^6 - 10^7$  GC cycles.

### III. RESULTS

#### A. Locating the critical point

Our first aim is to locate the critical point of the transition. To this end, it is convenient to consider how the shape of the distribution  $P(m)$  changes with the fugacity. In the bulk, we recover the behavior typical of a critical transition. At high fugacity,  $P(m)$  is bimodal with two well-resolved peaks, indicating two-phase coexistence. At low fugacity,  $P(m)$  is a single peak centered around  $m = 0$ . At intermediate fugacities, the system becomes critical, where  $P(m)$  remains bimodal, but with overlapping peaks. The critical fugacity  $z_{\text{cr}}$  is obtained via the Binder cumulant

$$U_4 = 1 - \frac{\langle m^4 \rangle}{3\langle m^2 \rangle^2}, \quad \langle m^p \rangle = \int_{-\infty}^{\infty} m^p P(m) dm, \quad (4)$$

which becomes  $L$ -independent at the critical point [35]. The result is shown in Fig. 1(a), where  $U_4$  is plotted as a function of  $z$ , for various system sizes  $L$ . The curves strikingly intersect, from which  $z_{\text{cr}}$  can be accurately extracted (Table II). At the critical point, not only the cumulant is scale invariant, but in fact the entire distribution  $P(m)$  [35, 36]

$$z = z_{\text{cr}} : \quad P(m) \propto P^*(a_m L^{\beta/\nu} m), \quad (5)$$

with  $\beta$  ( $\nu$ ) the critical exponent of the order parameter (correlation length),  $P^*(x)$  a scaling function that does not depend on system size, and constant  $a_m$ . The critical exponents, as well as  $P^*(x)$ , are characteristic of the

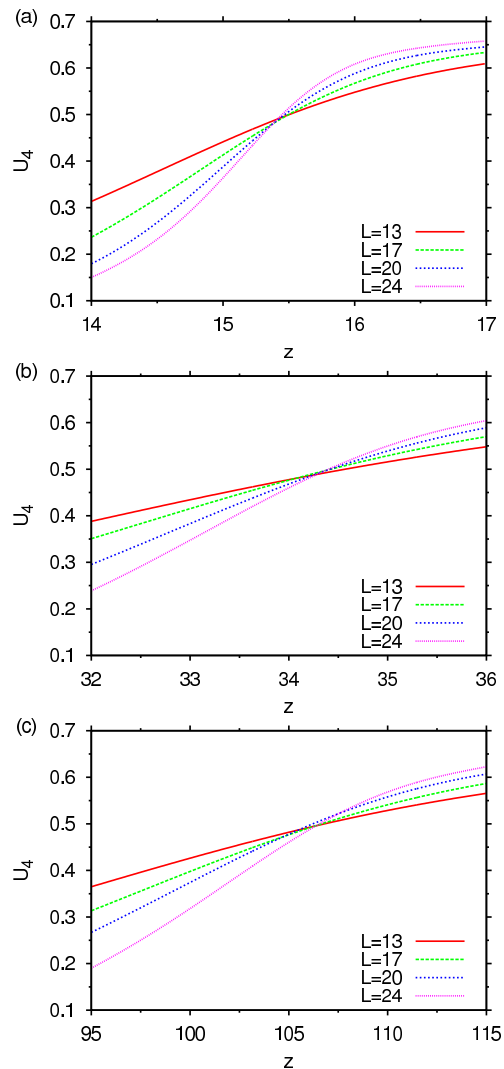


FIG. 1: Binder cumulant  $U_4$  as a function of the fugacity  $z$  for different system sizes  $L$ . The upper panel (a) shows the bulk result. Panels (b) and (c) show the result obtained in the presence of the porous medium, at medium density  $\rho_M = 0.1$  and  $0.2$ , respectively. The intersection of the curves for different  $L$  yields the critical fugacity  $z_{\text{cr}}$  (Table II).

universality class. We provide numerical estimates of the critical exponents for bulk Ising and RIM universality in Table I. In Fig. 2(a), we plot  $P(m)$  obtained at criticality, but with the horizontal axis scaled conform Eq. (5), using bulk Ising exponents. We observe that the data for different  $L$  collapse, consistent with an Ising critical point. However, one should regard these observations with some caution, as the critical properties of the RIM are very similar. In fact, the exponent ratio  $\beta/\nu$  is essentially identical between the two classes (and the same holds for  $\gamma/\nu$ , with  $\gamma$  the susceptibility critical exponent). Therefore, while the data clearly show the presence of a critical point, they do not unambiguously identify the universality class (although for the bulk case, there is no

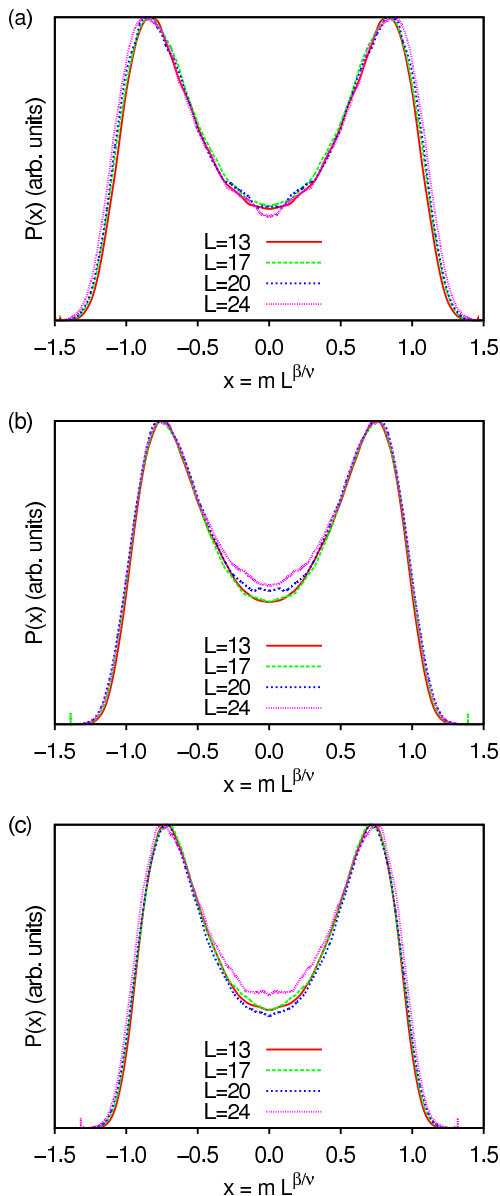


FIG. 2: The distribution  $P(m)$  obtained at the critical fugacity  $z = z_{\text{cr}}$  for various system sizes  $L$  and scaled conform Eq. (5). The upper panel (a) shows the bulk result ( $\rho_M = 0$ ) using bulk Ising critical exponents. Panels (b) and (c) show the result obtained in the presence of the porous medium, at medium density  $\rho_M = 0.1$  and  $0.2$ , respectively, where RIM critical exponents were used. Note that, in all panels, the distributions were explicitly symmetrized “by hand” after the simulation had completed.

reason to doubt Ising universality [29, 31, 37].

In the presence of the porous medium, the behavior of  $P(m)$  is similar, and a critical point can still be identified. The only complication is that results must be meaningfully averaged over the  $M \geq 100$  medium configurations. In contrast to the RFIM [8, 10], we observed that the peak positions in  $P(m)$  did not fluctuate much

TABLE II: Critical point properties of the fluid mixture confined to a neutral porous medium of density  $\rho_M$  obtained in this work. Listed are the critical fugacity  $z_{\text{cr}}$ , and the critical density  $\rho_{\text{cr}}$ .

$\rho_M$	$z_{\text{cr}}$	$\rho_{\text{cr}}$
0	15.42	0.430
0.1	34.09	0.403
0.2	105.6	0.379

between different configurations of the porous medium. For this reason, the probability distributions were simply averaged to yield the disorder averaged distribution

$$[P(m)] \equiv \frac{1}{M} \sum_{i=1}^M P^{(i)}(m), \quad (6)$$

where  $i$  labels the medium configurations. The cumulant analysis of  $[P(m)]$  is presented in Fig. 1(b) and (c), for  $\rho_M = 0.1$  and  $0.2$ , respectively. We again observe that curves for different  $L$  intersect, enabling rather accurate estimates of  $z_{\text{cr}}$  (Table II). The scaling of  $[P(m)]$  at criticality is confirmed in the corresponding panels of Fig. 2, where the critical exponents of the RIM were used. Again, we emphasize that this analysis accurately locates the critical point, but it does not warrant conclusions concerning the universality class.

We also estimated the critical density  $\rho_{\text{cr}}$ . To this end, we monitored how the density  $\rho_L$  varied with the system size  $L$ , with  $\rho_L$  obtained in the finite system at the critical fugacity  $z = z_{\text{cr}}$ . The latter were subsequently extrapolated to the thermodynamic limit using  $\rho_{\text{cr}} - \rho_L \propto 1/L$ . We thus ignore any singular behavior in  $\rho_{\text{cr}}$ , which is justified for our purposes since the shift  $\rho_{\text{cr}} - \rho_L$  is typically small. The resulting estimates of  $\rho_{\text{cr}}$  are reported in Table II. Our estimate of the bulk critical density compares well to  $\rho_{\text{cr}} = 0.4299$  obtained in semi-grand canonical simulations [29]. Note that, while  $z_{\text{cr}}$  increases with  $\rho_M$ ,  $\rho_{\text{cr}}$  decreases. The increase of  $z_{\text{cr}}$  conforms to “Kelvin-like” behavior, i.e. a suppression of the transition temperature upon increasing confinement. The decrease of  $\rho_{\text{cr}}$  most likely reflects the fact that an increasing fraction of space is occupied by the quenched particles.

## B. Correlation length critical exponent

We now attempt to measure the critical exponent  $\nu$  of the correlation length, using the finite-size scaling approach of Ref. 38. To this end, we select two of our data sets, corresponding to different system sizes,  $L_1$  and  $L_2$ . We then vary the fugacity, and plot the cumulant  $y = U_4(L_2)$  of the system with size  $L_2$  versus  $x = U_4(L_1)$  of the system with size  $L_1$  (the curve is thus parametrized by the fugacity  $z$ ). An example is provided in Fig. 3. The critical point corresponds to the fixed-point condition  $U_4(L_1) = U_4(L_2)$ , i.e. where the curve

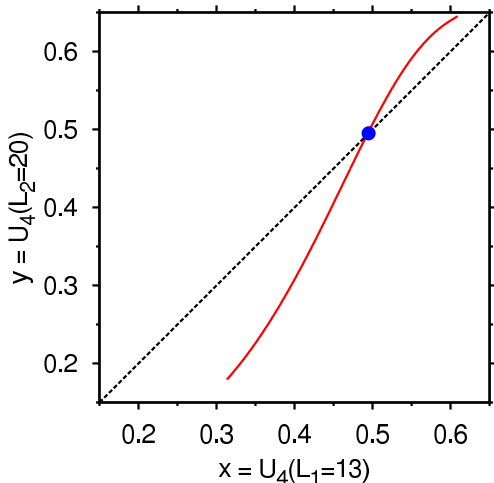


FIG. 3: Demonstration of the method of Ref. 38 to determine the correlation length critical exponent  $\nu$  (data refer to the bulk system). The solid curve shows the cumulant of the system with size  $L_2$ , versus the cumulant of the system with size  $L_1$ . The intersection of this curve with the line  $y = x$  (dashed) marks the critical point (dot). The slope  $s$  of the solid curve at the critical point is related to  $\nu$  via Eq. (7).

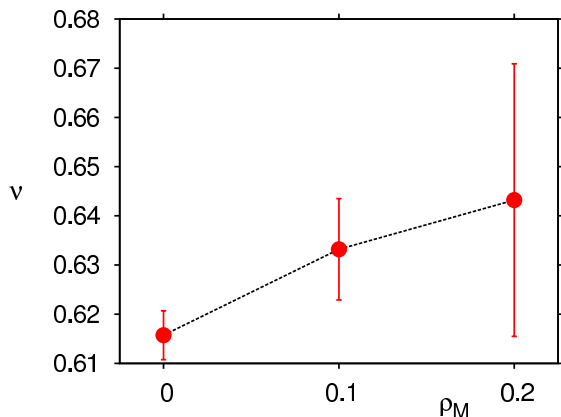


FIG. 4: The correlation length critical exponent  $\nu$  versus the density of the porous medium  $\rho_M$ , as obtained using the method of Ref. 38. The data reveal that  $\nu$  inside the porous medium exceeds the bulk value, in qualitative agreement with RIM universality.

$y(x)$  intersects the line  $y = x$  (indicated by the dot). The correlation length critical exponent is determined by the slope  $s = y'(x)$  evaluated at the fixed point

$$\nu = \ln b / \ln s, \quad b = L_2/L_1. \quad (7)$$

Since  $y(x)$  is essentially linear around the fixed-point, the slope  $s$  can be determined rather accurately.

In Fig. 4, we plot the resulting estimates of  $\nu$  versus  $\rho_M$ . Since, for each value of  $\rho_M$ , we have data for four different system sizes, a total of six measurements could be made each time. The dots in Fig. 4 show the average of these measurements, while the error bars reflect

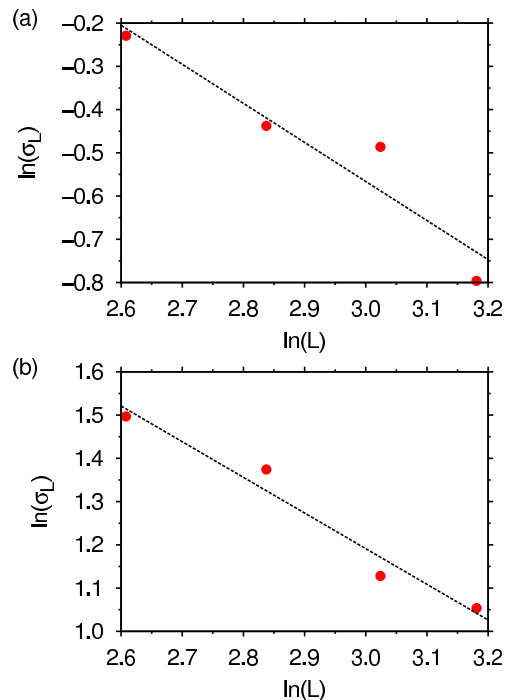


FIG. 5: The decay of the fluctuation  $\ln \sigma_L$  in the pseudo-transition points (defined via the maximum of the susceptibility) as a function of  $\ln L$ , for porous medium densities  $\rho_M = 0.1$  (a) and  $\rho_M = 0.2$  (b). The data are approximately linear, indicating a power law decay  $\sigma \propto 1/L^k$ , with  $k \sim 0.9$  obtained by fitting (dashed lines).

the standard error. Clearly, the errors are rather large. However, we do observe that  $\nu$  inside the porous medium ( $\rho_M > 0$ ) is larger than its bulk ( $\rho_M = 0$ ) value, a trend which is at least qualitatively consistent with RIM universality.

In principle, a similar analysis can also be used to determine the critical exponent ratio  $\beta/\nu$  [39]. However, as mentioned before, the latter is essentially identical for the Ising and RIM universality class, and so we did not pursue this.

### C. Distribution of pseudo-transition points

We now consider the distribution of pseudo-transition points; the latter are frequently encountered in systems containing quenched disorder, and their analysis has attracted much attention [40–44]. To be specific, in a finite system of size  $L$ , the fugacity  $z_{L,i}$  where the system becomes pseudo-critical, fluctuates between the  $i = 1, \dots, M$  realizations of the porous medium (the term pseudo-critical is used because a finite system never becomes truly critical, of course). The pseudo-critical fugacity  $z_{L,i}$  may be defined as the fugacity where the susceptibility

$$\chi_{L,i} = V(\langle m^2 \rangle - \langle |m| \rangle^2), \quad (8)$$

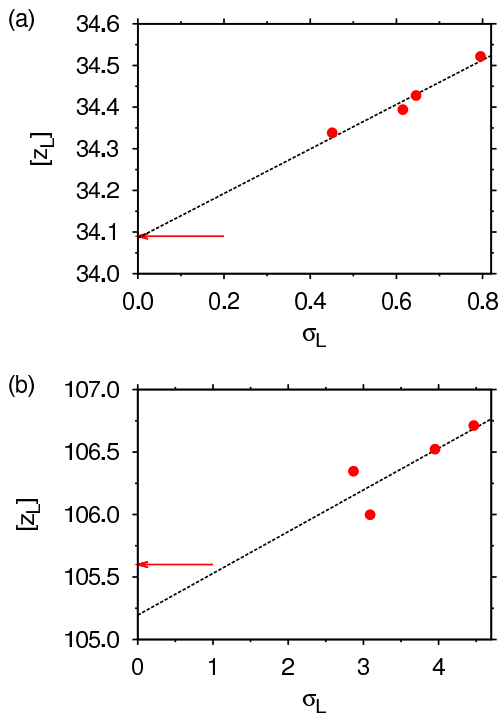


FIG. 6: Variation of  $[z_L]$  with  $\sigma_L$ , for  $\rho_M = 0.1$  (a) and  $\rho_M = 0.2$  (b). The dashed lines are linear fits, whose intercept corresponds to  $z_{cr}$ . The arrows indicate the estimates of  $z_{cr}$  obtained from cumulant intersections.

reaches its maximum, as measured in the  $i$ -th realization of the porous medium, and with  $m$  given by Eq. (2).

The key question is how the disorder fluctuation

$$\sigma_L^2 = [z_L^2] - [z_L]^2, \quad [z_L^p] = \frac{1}{M} \sum_{i=1}^M z_{L,i}^p, \quad (9)$$

decays with the system size  $L$ . In general, one expects a power law decay:  $\sigma_L \propto 1/L^k$ , with  $k > 0$ . According to the Brout argument  $k = d/2$ , with  $d$  the spatial dimension [45]. The Brout argument is correct, provided the correlation length is finite, such that the system will eventually self-average. However, at a critical point, the correlation length is infinite, and self-averaging is violated. In that case, the fluctuations decay slower,  $k = 1/\nu$ , with  $\nu$  the critical exponent of the correlation length [42, 43]. Note that, since fluctuations may never decay faster than self-averaging, an interesting inequality  $\nu > 2/d$  is implied [46, 47].

In Fig. 5, we show how  $\sigma_L$  decays with  $L$ , for both densities of the porous medium. Note that a double-logarithmic scale is used. The data are compatible with a power law decay. In addition, the exponent of the decay,  $k \sim 0.9$ , is smaller than  $d/2 = 1.5$ , showing that self-averaging is violated, which is indeed expected for RIM universality. The actual exponent values are, however, rather far removed from RIM values (as were our  $\nu$  estimates of Fig. 4). We believe the most likely explana-

tion is the limited number of porous medium realizations that we could simulate, and so  $\sigma_L$  could not be determined very accurately.

The fact that  $\sigma_L \propto 1/L^{1/\nu}$  is also interesting in relation to the average pseudo-transition point  $[z_L]$ , whose shift from its thermodynamic limit value  $z_{cr}$  is given by the same form:  $z_{cr} - [z_L] \propto 1/L^{1/\nu}$ . Consequently, a graph of  $[z_L]$  versus  $\sigma_L$  should be linear, with the intercept corresponding to  $z_{cr}$ . The result is shown in Fig. 6, for both densities of the porous medium. The arrows indicate the estimates of  $z_{cr}$  obtained from the cumulant intersections of Fig. 1. While for  $\rho_M = 0.1$  the agreement between both methods is very reasonable, the data for  $\rho_M = 0.2$  reveal significant scatter. Nevertheless, the discrepancy remains within 1 %, and so we conclude that the expected scaling is confirmed.

#### IV. DISCUSSION

In this work, we have considered the critical behavior of a fluid confined to a random porous medium consisting of neutral walls. Our aim was to confirm the universality class of the corresponding liquid-vapor transition, expected to be the one of the random Ising model. While it remains extremely difficult to accurately obtain critical exponents for this *off-lattice* system, evidence of random Ising behavior is revealed by the disorder fluctuations. By monitoring the fluctuations in the pseudo-transition temperatures between different realizations of the porous medium, clear violations of self-averaging are observed. Within the limitations of our data, these disorder fluctuations were seen to scale with the system size as would be expected for the random Ising model. Also the trend of the critical exponent  $\nu$  associated to the divergence of the correlation length is compatible with the critical behavior of the random Ising model. Nevertheless, it is clear that much more computer power would be needed to reach the accuracy levels typical of lattice spin models [48]. We surmise that for such a high-resolution study the disorder averages should be calculated over several thousands realizations of the quenched disorder, whereas the present study adopted a few hundreds samples only.

For such a possible future study, it is advisable to restrict  $\rho_M \sim 0.1$  or so. This value is large enough to induce random Ising effects, yet small enough to avoid the severe equilibration problems that set in at higher medium densities. Another quantity that would also be interesting to monitor is the coexistence diameter [49]. Following the Harris criterion [16], the critical exponent of the specific heat  $\alpha$  is negative for the random Ising model, but positive for the bulk Ising model. Such a change in sign might yield a more pronounced numerical signature in simulation data.

## Acknowledgments

R.V. acknowledges financial support by the German research foundation (Emmy Noether grant VI 483). G.P.

acknowledges the National Research Foundation (NRF) for financial support through Grant No. 80795.

- 
- [1] P. Wiltzius, S. B. Dierker, and B. S. Dennis, *Phys. Rev. Lett.* **62**, 804 (1989).
- [2] A. P. Y. Wong and M. H. W. Chan, *Phys. Rev. Lett.* **65**, 2567 (1990), URL <http://dx.doi.org/10.1103/physrevlett.65.2567>.
- [3] A. P. Y. Wong, S. B. Kim, W. I. Goldberg, and M. H. W. Chan, *Phys. Rev. Lett.* **70**, 954 (1993), URL <http://dx.doi.org/10.1103/physrevlett.70.954>.
- [4] Y. B. Melnichenko, G. D. Wignall, D. R. Cole, and H. Frielinghaus, *Phys. Rev. E* **69**, 057102 (2004).
- [5] J. V. Maher, W. I. Goldberg, D. W. Pohl, and M. Lanz, *Phys. Rev. Lett.* **53**, 60 (1984).
- [6] P. G. De Gennes, *J. Phys. Chem.* **88**, 6469 (1984), URL <http://dx.doi.org/10.1021/j150670a004>.
- [7] T. Nattermann, in *Spin Glasses and Random Fields*, edited by A. P. Young (World Scientific, Singapore, 1998), p. 277, URL <http://xxx.lanl.gov/abs/cond-mat/9705295>.
- [8] R. L. C. Vink, T. Fischer, and K. Binder, *Phys. Rev. E* **82**, 051134 (2010), URL <http://dx.doi.org/10.1103/physreve.82.051134>.
- [9] R. L. C. Vink, K. Binder, and H. Löwen, *Phys. Rev. Lett.* **97**, 230603 (2006).
- [10] R. L. C. Vink, K. Binder, and H. Löwen, *J. Phys.: Condens. Matter* **20**, 404222 (2008).
- [11] T. Fischer and R. L. C. Vink, *J. Phys.: Condens. Matter* **23**, 234117 (2011), ISSN 0953-8984, URL <http://dx.doi.org/10.1088/0953-8984/23/23/234117>.
- [12] T. Fischer and R. L. C. Vink, *J. Chem. Phys.* **134**, 055106 (2011), URL <http://dx.doi.org/10.1063/1.3530587>.
- [13] E. Kierlik, M. L. Rosinberg, G. Tarjus, and E. Pitard, *Molecular Physics* **95**, 341 (1998).
- [14] P. D. S. Lucentini and G. Pellicane, *Phys. Rev. Lett.* **101**, 244973 (2008).
- [15] M. Hasenbusch, F. P. Toldin, A. Pelissetto, and E. Vicari, *Journal of Statistical Mechanics: Theory and Experiment* **2007**, P02016+ (2007), ISSN 1742-5468, URL <http://de.arxiv.org/abs/cond-mat/0611707>.
- [16] A. B. Harris, *J. Phys. C* **7**, 1671 (1974), ISSN 0022-3719, URL <http://dx.doi.org/10.1088/0022-3719/7/9/009>.
- [17] W. G. Madden and E. D. Glandt, *J. Stat. Phys.* **51**, 537 (1988), URL <http://dx.doi.org/10.1007/bf01028471>.
- [18] W. G. Madden, *J. Chem. Phys.* **96**, 5422 (1992), URL <http://scitation.aip.org/getabs/servlet/GetabsServlet?prog=normal&id=JCPA6000096000007005422000001&idtype=cvips&gifs=yes>.
- [19] J. Given and G. Stell, *Physica A: Statistical and Theoretical Physics* **209**, 495 (1994), ISSN 03784371, URL [http://dx.doi.org/10.1016/0378-4371\(94\)90200-3](http://dx.doi.org/10.1016/0378-4371(94)90200-3).
- [20] E. Lomba, J. A. Given, G. Stell, J. J. Weis, and D. Levesque, *Phys. Rev. E* **48**, 233 (1993).
- [21] K. S. Page and P. A. Monson, *Phys. Rev. E* **54**, 6557 (1996), URL <http://dx.doi.org/10.1103/PhysRevE.54.6557>.
- [22] M. Alvarez, D. Levesque, and J. J. Weis, *Phys. Rev. E* **60**, 5495 (1999).
- [23] Y. Duda, O. Pizio, and S. Sokolowski, *J. Phys. Chem.* **108**, 19442 (2004).
- [24] E. Pitard, M. L. Rosinberg, G. Stell, and G. Tarjus, *Phys. Rev. Lett.* **74**, 4361 (1995).
- [25] L. Sarkisov and P. A. Monson, *Phys. Rev. E* **61**, 7231 (2000), URL <http://dx.doi.org/10.1103/physreve.61.7231>.
- [26] E. Schöll-Paschinger, D. Levesque, J. J. Weis, and G. Kahl, *Phys. Rev. E* **64**, 011502 (2001), URL <http://dx.doi.org/10.1103/physreve.64.011502>.
- [27] G. Pellicane, C. Caccamo, D. S. Wilson, and L. L. Lee, *Phys. Rev. E* **69**, 061202 (2004).
- [28] L. Sarkisov and P. R. van Tassel, *J. Chem. Phys.* **123**, 164706 (2005).
- [29] W. Gózdź, *J. Chem. Phys.* **119**, 3309 (2003).
- [30] D. P. Landau and K. Binder, *A Guide to Monte Carlo Simulations in Statistical Physics* (Cambridge University Press, Cambridge, 2000).
- [31] N. B. Wilding, *Phys. Rev. E* **67**, 52503 (2003).
- [32] D. Frenkel and B. Smit, *Understanding Molecular Simulation* (Academic Press, San Diego, 2001).
- [33] A. M. Ferrenberg and R. H. Swendsen, *Phys. Rev. Lett.* **61**, 2635 (1988), URL <http://dx.doi.org/10.1103/physrevlett.61.2635>.
- [34] A. Pelissetto and E. Vicari, *Phys. Rep.* **368**, 549 (2002).
- [35] K. Binder, *Z. Phys. B* **43**, 119 (1981), ISSN 0340-224X, URL <http://dx.doi.org/10.1007/bf01293604>.
- [36] N. B. Wilding, *J. Phys.: Condens. Matter* **9**, 585 (1997), URL <http://dx.doi.org/10.1088/0953-8984/9/3/002>.
- [37] J. Köfinger, N. B. Wilding, and G. Kahl, *J. Chem. Phys.* **125**, 234503 (2006).
- [38] K. Kaski, K. Binder, and J. D. Gunton, *Phys. Rev. B* **29**, 3996 (1984), URL <http://dx.doi.org/10.1103/physrevb.29.3996>.
- [39] W. Rzyso, J. J. de Pablo, and S. Sokolowski, *J. Chem. Phys.* **113**, 9772 (2000).
- [40] K. Bernardet, F. Pázmándi, and G. G. Batrouni, *Phys. Rev. Lett.* **84**, 4477 (2000), URL <http://dx.doi.org/10.1103/physrevlett.84.4477>.
- [41] S. Wiseman and E. Domany, *Phys. Rev. Lett.* **81**, 22 (1998), URL <http://dx.doi.org/10.1103/physrevlett.81.22>.
- [42] S. Wiseman and E. Domany, *Phys. Rev. E* **58**, 2938 (1998), cond-mat/9802102, URL <http://arxiv.org/abs/cond-mat/9802102>.
- [43] A. Aharony and A. B. Harris, *Phys. Rev. Lett.* **77**, 3700 (1996), URL <http://dx.doi.org/10.1103/physrevlett.77.3700>.
- [44] C. Monthus and T. Garel, *Eur. Phys. J. B* **48**, 393 (2005), ISSN 1434-6028, URL <http://dx.doi.org/10.1140/epjb/e2005-00417-7>.

- [45] R. Brout, Phys. Rev. **115**, 824 (1959), URL <http://dx.doi.org/10.1103/physrev.115.824>.
- [46] A. Aharony, A. B. Harris, and S. Wiseman, Phys. Rev. Lett. **81**, 252 (1998), URL <http://dx.doi.org/10.1103/physrevlett.81.252>.
- [47] J. T. Chayes, L. Chayes, D. S. Fisher, and T. Spencer, Phys. Rev. Lett. **57**, 2999 (1986), URL <http://dx.doi.org/10.1103/physrevlett.57.2999>.
- [48] P. Theodorakis and N. Fytas, The European Physical Journal B - Condensed Matter and Complex Systems **81**, 245 (2011), ISSN 1434-6028, URL <http://dx.doi.org/10.1140/epjb/e2011-20091-4>.
- [49] R. L. C. Vink, J. Chem. Phys. **124**, 094502 (2006), URL <http://scitation.aip.org/getabs/servlet/GetabsServlet?prog=normal&id=JCPA6000124000009094502000001&idtype=cvips&gifs=yes>.